Lasers in Manufacturing Conference 2021

Determination of the beam position in laser deep penetration welding using coaxially acquired images of the keyhole front and machine learning

Pablo Dilger[a,b,*], Carola Forster[a], Elias Klein[a], Silvana Burger[a,b], Eric Eschner[a,b], Michael Schmidt[a,b]

[a]*Institute of Photonic Technologies (LPT), University of Erlangen-Nuremberg (FAU), Konrad-Zuse-Straße 3/5, 91052 Erlangen, Germany*
[b]*Erlangen Graduate School in Advanced Optical Technologies (SAOT), University of Erlangen-Nuremberg (FAU), Paul-Gordan-Straße 6, 91052 Erlangen, Germany*

Abstract

The joining technology of laser beam welding offers high flexibility and productivity. However, the small laser beam focus demands dependable quality assurance to ensure a sufficient connection of the parts. In keyhole welding of metal sheets in butt joint configuration, a gap is visible at the keyhole front, which correlates with the leading joint position. This process feature can be used for quality control by arranging a high-speed camera coaxially to the laser beam to monitor the keyhole. Here, we present a machine learning approach for a robust determination of the beam position relative to the joint based on the keyhole front morphology. For this purpose, we conducted a series of experiments to produce a set of labeled images, which are used to train a convolutional neural network. After training on the data, the network can predict the position of the keyhole front gap, setting the foundation for a quality control system.

Keywords: laser deep penetration welding; machine learning; image processing; quality assurance

1. Introduction

Laser keyhole welding in comparison to other welding processes is characterized by a small heat affected zone due to the high intensity of the focused laser beam, offering welds with a high aspect ratio. However, the

* Corresponding author. Tel.: +49 9131 85-23245; fax: +49 9131 85-23234 .
E-mail address: pablo.dilger@lpt.uni-erlangen.de .

small spot size demands low tolerances in terms of lateral beam position, especially in the case of welding parts in butt joint configuration. For this reason, reliable seam tracking techniques and systems for quality assurance are necessary to ensure a sufficient connection of the parts. Conventional seam tracking techniques use optical sensors to measure the joint geometry. For example optical coherence tomography (OCT) can be used to acquire the workpiece topography pre- and post-process enabling the tracking of the joint and measure the weld bead as shown by Dupriez and Truckenbrodt, 2016. However, OCT systems require a pronounced characteristic within the topography of the joint, which limits applicability in butt joint configuration with a technical zero gap. Another approach is to use additional illumination and a camera to detect the joint. Kos et al., 2019 exploited the fact that the gap in butt joint configuration reflects less light compared to the bare metal sheet allowing the detection of the joint by means of image processing. Disadvantages of both the OCT system and camera based approach with additional illumination is the pre-process measurement of the joint, which means that subsequent deviations due to thermal movement of the workpiece or lateral displacement of the processing optic cannot be compensated for as mentioned by Regaard et al., 2009. In addition, with these techniques, the actual beam position is not accessible during the process, resulting in a limited use for monitoring the connection quality.

We identified a visible gap in the thermal emissions of the keyhole front when welding in butt joint configuration, which can be coaxially monitored with a high-speed camera. Since this gap correlates with the preceding joint gap, the feature can be used within a closed-loop control for beam positioning as shown in Dilger et al., 2020. However, the manifestation of the control feature depends on the melt dynamics at the keyhole front, mainly influenced by the process parameters. If the primary feature, the melt gap at the front, is less pronounced, our previously proposed algorithm in Dilger el al., 2020 cannot reliably determine the position. This shortcoming is addressed in this work by a machine learning approach, allowing the consideration of secondary features within the image. The approach proves to deliver a more reliable detection of the keyhole front gap independent of the keyhole shape and front gap morphology.

2. Methods

This section first describes the experimental setup and process for image data generation. Secondly, the procedure for data labeling is presented since we used a supervised learning approach. Finally, the machine learning method for predicting the position of the keyhole front gap is described.

2.1. Experiments

For the experiments we used the same setup described in a previous work in Dilger et al., 2020. The experiments were conducted with a TruDisk6001 laser beam source with a wavelength of 1030 nm and a maximum output power of 6 kW. A Precitec YW52 processing optics with an imaging port for coaxial observation of the process zone was used for focusing the beam, resulting in a spot diameter of 600 µm. Relative movement between the laser beam and the workpiece was realized with a two-axis stage system (Aerotech Pro280LM). The thermal emissions of the process zone were imaged with a magnification of 2.15 and captured with a high-speed camera (Mikrotron EoSens 3CXP) with a frame rate of 3 kHz at 512x512 pixels.

To obtain a broad data basis with different keyhole shapes we varied the used materials and process parameters over a wide parameter space, listed in Table 1. The combination of laser power and feed rate was selected such that keyhole welding with a welding depth of at least 1 mm occurred. The metal sheets were arranged in a butt joint configuration with a technical zero gap. A total of 81 experiments were carried out with different parameter and material combinations. The beam path on the metal sheets was a diagonal line across the joint, as depicted in Fig. 1 (a). The weld length in y-direction was set to 100 mm, whereas the lateral

movement of the beam in x-direction across the joint gap was set to 0.8 mm. By this means, it is possible to generate an image data set with different and predefined beam positions relative to the joint, which is advantageous regarding the data labeling procedure (see section 2.2). Fig. 1 (b) shows three coaxially acquired high-speed images of the process zone at different positions with respect to the beam path. The respective beam position relative to the joint correlates with the gap position at the keyhole front.

Table 1. Process parameters and materials used in the experiments.

Process parameter / material	
Sheet thickness	1 and 3 mm
Sheet material	Stainless steel (1.4541), zinc coated steel (DX56)
Laser power	1 – 6 kW
Feed rate	33 – 200 mm s^{-1}

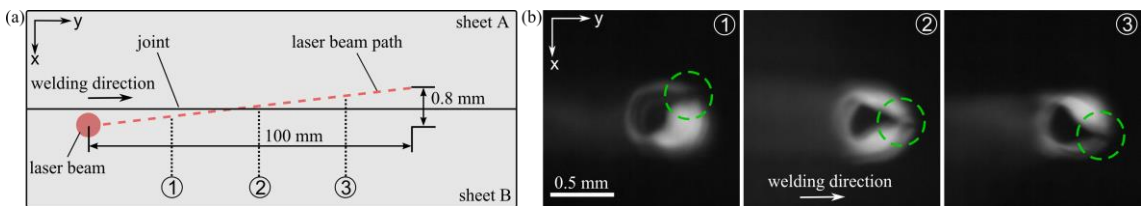

Fig. 1. (a) Laser beam path during the experiments with a weld length of 100 mm in y-direction and a lateral movement across the joint of 0.8 mm in x-direction. (b) Three coaxially acquired process images showing the keyhole with the control feature at the front marked with a green circle. The images are assigned to the respective beam positions in (a).

2.2. Data labeling procedure

Form the acquired image data described in section 2.1 the positions of the keyhole front gap of each image have to be determined and integrated in a data set, to be used as ground truth within a convolutional neural network (CNN), see section 2.3. Since manual data labeling of a large number of images would be very costly and time-consuming, a semi-automated procedure was developed. At first, an image processing algorithm for an initial determination of the keyhole front gap positon was used. The algorithm calculates intensity profiles along circular arcs with a central angle of 100° and different radii aligned in feed direction. The position of the minimum intensity value within the profiles usually corresponds to the front gap and is therefore taken as gap position, provided it satisfies predefined thresholds. Since the intensity profiles are calculated in a polar coordinate system, the respective coordinates of the minimum intensity value must be converted to Cartesian coordinates to determine the lateral offset. Considering the feed direction on the y-axis, the x-value of the calculated gap coordinates describes the offset between gap position and keyhole center or beam center. A detailed description of the image processing algorithm is given in Dilger et al., 2020.

In Fig. 2, the lateral offset in micrometer is shown as a function of the image number for two experiments. If the image processing algorithm is able to detect the keyhole front gap, its position is indicated with a blue dot, while the red dots denote a lacking detection. The detected positions refer to the diagonal crossing of the joint during welding as described in section 2.1. Due to the differing visibility of the keyhole front gap, the quantity of the detected positions varies. Since the outcome of a machine learning algorithm would not improve the detection if only the detected positions of the image processing algorithm are integrated in the labeled data set, the missing positions must be determined. For this reason, a linear function is fitted to the

detected front gap positions as indicated by the solid line in Fig. 2. The fitting procedure takes the feed rate, the frame rate of the camera and the beam path used in the corresponding experiment into account. With the knowledge of these parameters, it is applicable to interpolate the missing gap positions with the fitted line. Additionally, potential erroneous detections are removed by this procedure. We used a fitting approach because the respective gap position could not be directly assigned to every image due to small deviations regarding the clamping device, the beam path, and the starting point of the experiment. For labeling the image data, the gap position of the respective image number is deduced from the fitted line and is saved as absolute pixel value in vertical direction (x-direction within the used coordinate system in Fig. 1). To ensure the ground truth of the data set does not incorporate incorrect labels the images are further examined manually. For this, the gap positions are plotted into the images to verify that the detected positions match the visible front gap. The dataset cleaned by this procedure includes approximately 40,000 images.

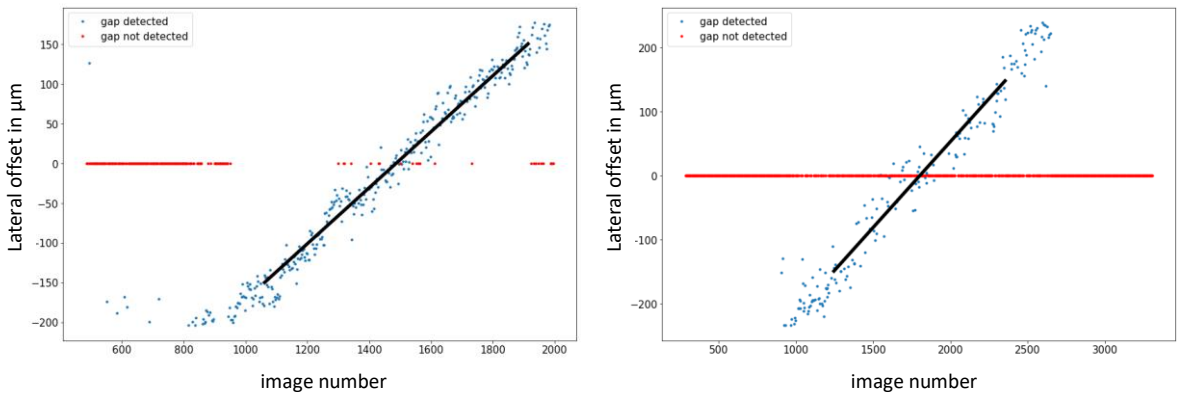

Fig. 2. Lateral offset determined by the image processing algorithm for two different experiments. Red dots indicate a lack of detection. The solid black line represents the result of the fitting procedure for data labeling.

2.3. Machine Learning method

For the improved detection method, CNN´s were chosen since this deep learning algorithm shows promising result for similar tasks as demonstrated by Gao and Zhang, 2014 and Zhang et al., 2019. Furthermore, their architecture is explicitly designed for image data as outlined by LeCun et al., 2015. To optimize the network structure different layer configurations and hyperparameter were investigated by comparing their performance with each other. In addition, different training approaches were evaluated with and without progressive resizing, which is explained below. In this work, we present the approach that showed the best prediction results.

In this supervised learning method a model is trained for mapping the captured images to the corresponding gap positions, which are determined as described in section 2.2. The target is to fit a model that reliably predicts the front gap position even for unknown data. The dataset was split randomly in 85 % training/validation set and 15 % test set. Training of the network was realized with progressive resizing, which can be used as a form of transfer learning to achieve better generalization and shorter training times, for example shown by Colangelo et al., 2020. In progressive resizing the CNN is trained at first with smaller images, which are then consecutively increased. To the prior trained network additional layers are added to be trained with the larger images. In the present work, the original images of size 512x512 pixels were reduced to sizes of 64x64, 128x128 and 256x256 pixels, which are then used for training in this order. The labels, respectively the gap positions,

were adjusted to the reduced image size accordingly. The input layer of the CNN consists of a convolutional layer with a shape according to the image size and a kernel size of 7x7. As pooling layer, maximal pooling with a filter size of 2x2 was used. Subsequently, several convolutional and maximal pooling layers were alternated, depending on the image size. The last layers of the network consist out of a flatten layer and dense layers. The RMSProp (root mean square propagation) optimizer was used to compile the model for training, for example applied by Mukkamala and Hein, 2017. The compiled models were evaluated in terms of mean absolute error (MAE) defined as:

$$\mathrm{MAE} = \frac{1}{n}\sum_{i=1}^{n}\left|\hat{Y}_i - Y_i\right| \qquad (1)$$

where $\hat{Y}_i$ is the model prediction, Y_i is the corresponding target value in pixel and n is the number of data pairs. As deep learning library, we used TensorFlow, which was implemented by using the Keras Application Programming Interface.

3. Results and discussion

As described in the previous section a CNN was trained with images of the process zone during keyhole welding acquired coaxially to the laser beam for the prediction of the front gap position. The results of the network configuration with the best prediction values are presented, trained with images of size 256x256 pixels and using progressive resizing. The training and validation MAE reached 1.5 pixel after training of the network. Evaluating the trained network on the test set containing unknown image data even resulted in a MAE of 1.3 pixels. Since the gap dimension is mostly several pixels wide, this value is within an acceptable range to obtain a reliable determination of the gap position. Considering the reduction of the image size, the pixel size of 8 µm and the magnification of the imaging system, the MAE on the object side is calculated to 9.7 µm. Using a laser spot diameter of 600 µm and thus welding with a keyhole size of comparable dimensions, this MAE is sufficient to determine the front gap position. Fig. 3 shows representative images from the test set in which the labeled gap positions and the positions predicted by the CNN are indicated by a green and blue line, respectively. The predicted gap positions agree very well with the labeled data for different keyhole shapes. Furthermore, the CNN correctly predicts the front gap position even for weakly pronounced front gaps, underlining the high performance of the network.

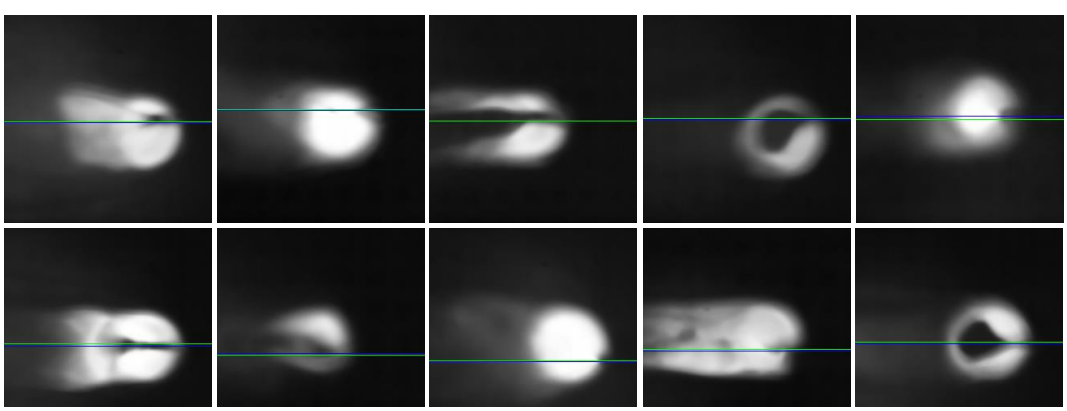

Fig. 3. Representative images from the test set with the respective label (green line) and network prediction (blue line) of the keyhole front gap position.

To investigate the CNN's performance for the determination of the gap position for a complete weld experiment, the predicted values for two experiments are shown as a function of the image number in Fig. 4. Here, Fig. 4 (a) represents an experiment with a noticeably and consistently pronounced keyhole front gap, while in Fig. 4 (b) the keyhole front gap varies between not visible and less visible as depicted by the process images. It must be mentioned that the analyzed images originate both from the training and test set as well as from data that was not included in the data basis. This means they contain images prior to initiation of the welding process, images in which the laser beam spot was not on the joint gap or images that were manually excluded from the data basis because no gap was visible to confirm a correct labeling by the fitting procedure. The period in which the beam focus was on the joint gap is shown with two vertical lines. Only in this range it is theoretically possible to determine the position of the joint gap relative to the beam. The graph in Fig. 4 (a) shows that the CNN can precisely predict the front gap position, as denoted by the linear slope of the predicted values in the relevant range (image number ~550 – 1,300). This behavior is consistent with the expectation due to the experimental procedure for image data generation described by a linear crossing of the joint. The graph in Fig. 4 (b), on the other hand, does not show the linear slope. However, a linear trend can be identified within the relevant range (image number ~1,000 – 2,500). This indicates that the network predicts the gap position at least for a part of the images correctly. The difference in the prediction performance for the two experiments derives from the varying visibility of the front gap. The more pronounced keyhole front gap in the first experiment results in better predictions of the network. Since in the second experiment the keyhole front gap is temporarily not visible, the predicted positions are less accurate. Images, where the gap is not visible, were excluded from the data basis because the label position could not be verified and therefore did not contribute to the fitting of the network model. Nevertheless, it is interesting that the network detects the correct sign of the lateral offset and is only erroneous in the quantification of the gap position. For example, taking the images from 1,000 – 1,700, the network only predicts gap positions from 120 – 145 pixels, meaning it predicts values on the correct keyhole side considering the welding direction. The reason for this could be that the CNN considers secondary features within the images that also contain information about the position of the keyhole front gap. These features are inherent image features and are visually not accessible compared to the primary feature, the keyhole front gap. Since the image processing algorithm described in section 2.2 does not access these secondary features, the CNN seems to be superior in this task. For images outside the relevant range, the CNN predicts the gap positions randomly since it has not been trained with images that do not contain the keyhole front gap. For this reason, the network has to be adjusted if images without a front gap are also to be detected.

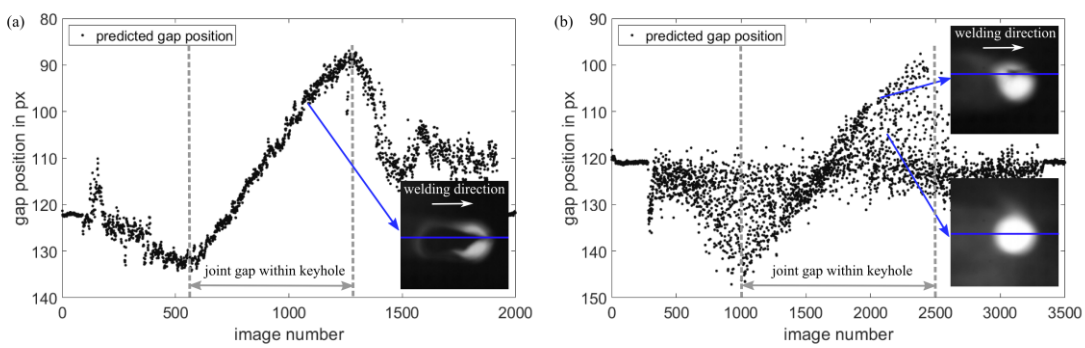

Fig. 4. Predicted gap positions by the CNN for two experiments. (a) Since the keyhole front gap is more pronounced, the predicted gap positions coincide with the expectation. (b) The temporarily absent keyhole front gap results in less accurate predictions ofthe network, however on the correct keyhole side considering the welding direction.

4. Conclusion

In the present paper, we have shown that by means of a knowledge-based image processing algorithm using a primary feature within the image, a machine learning approach based on CNNs can be developed that exploits image features that are not directly identifiable. These secondary features lead to a more reliable detection of the keyhole front gap, improving process-monitoring capabilities. Since the inherent image features are not visually accessible, this procedure should be thoroughly investigated in future work to determine which image features contribute to the prediction process of the CNN. We plan to investigate the generalizability of the CNN for other processing optics and welding configurations. With that, the responsible image features are also to be examined, allowing potentially the adjustment of the system design or welding configuration to better visualize these features and thus further improve the performance of the network. In addition, we plan to adjust the network model to detect images without a visible keyhole front gap to minimize random predictions. Since the mechanism leading to a visible keyhole front gap are not yet fully understood, especially the influence of the different process parameters, we also plan to conduct further experiments to investigate this interaction.

Acknowledgements

The authors gratefully acknowledge funding of the Erlangen Graduate School in Advanced Optical Technologies (SAOT) by the Bavarian State Ministry for Science and Art. We also thankfully acknowledge funding by the Bavarian State Ministry of Economic Affairs, Regional Development and Energy as part of the Bavarian research and development funding program "Elektronische Systeme".

References

Colangelo, F., Battisti, F., Neri, A., 2020. Progressive Training Of Convolutional Neural Networks For Acoustic Events Classification, in: 28th European Signal Processing Conference (EUSIPCO 2020). Amsterdam, the Nederlands.

Dilger, P., Eschner, E., Schmidt, M., 2020. Camera-based closed-loop control for beam positioning during deep penetration welding by means of keyhole front morphology. Procedia CIRP 94, p. 758–762.

Dupriez, N. D., Truckenbrodt, C., 2016. OCT for Efficient High Quality Laser Welding. Laser Technik Journal 13 (3), p. 37–41.

Gao, XD., Zhang, YX., 2014. Prediction model of weld width during high-power disk laser welding of 304 austenitic stainless steel. International Journal of Precision Engineering and Manufacturing 15 (3), p. 399–405.

Kos, M., Arko, E., Kosler H., Jezeršek, M., 2019. Remote laser welding with in-line adaptive 3D seam tracking. The International Journal of Advanced Manufacturing Technology 103 (9), p. 4577-4586.

LeCun, Y., Bengio, Y., Hinton, G., 2015. Deep learning. Nature 521 (7553), p. 436–444.

Mukkamala, M. C., Hein, M., 2017. Variants of RMSProp and Adagrad with Logarithmic Regret Bounds, 34th International Conference on Machine Learning, p. 2545–2553.

Regaard, B., Kaierle, S., Poprawe, R., 2009. Seam-tracking for high precision laser welding applications—Methods, restrictions and enhanced concepts, Journal of Laser Applications 21 (4), p. 183.

Zhang, Y., You, D., Gao, X., Zhang, N., Gao, P., 2019. Welding defects detection based on deep learning with multiple optical sensors during disk laser welding of thick plates. Journal of Manufacturing Systems 51, p. 87-94.